DEVELOPMENT OF DUCTILE CEMENTITIOUS MATERIALS WITH WOOD FIBRES

SIERRA BELTRAN, M. GUADALUPE; SCHLANGEN, ERIK

Microlab, M & E, Faculty of Civil Engineering and Geosciences, Delft University of Technology, P.O.Box 5048, 2600 GA Delft, The Netherlands

ABSTRACT

Wood fibres are studied as reinforcement for ductile cementitious materials. While much research has analyzed the properties of wood fibre-reinforced thin sheets elements and boards this paper presents the development of a material with enhanced ductility as well as low production cost (compared to synthetic fibre-reinforced concrete) that can be used for structural applications. For this purpose the properties of short wood fibres randomly oriented, a cement matrix and the fibre-matrix interface are engineered using a micromechanical based model. This paper summarizes the essential theoretical guidelines for this model and the laboratory tests done to evaluate the fibres and matrix properties.

KEYWORDS

Wood fibres; cement; ductility; micromechanics.

INTRODUCTION

Wood fibres are proposed as primary reinforcement in cement matrixes for structural applications. These natural fibres from vegetable origin are a renewable resource which price is only about 10% of the price of synthetic fibres currently used as reinforcement and require 70% less energy to be prepared. However, though wood fibres and synthetic fibres have similar values of modulus of elasticity, wood fibres have only half the tensile strength. These wood fibres have been studied and used to reinforce mortars for thin sheets and non structural applications where shrinkage control is useful. A literature review of research done with wood and other natural fibres showed the increase in flexural strength and toughness in cement pastes reinforced with wood fibres. This paper proposes a new approach to be able to tailor a ductile cementitious wood fibre reinforced material that could be used beyond non structural applications taking into account all the advantages of wood fibres as well as the possible disadvantage of a lower strength. The fibres, the matrix and the matrix-fibre interface are studied and after which the combined effect of these material constituents will be linked to the composite properties through micromechanics, leading to the new material design.

MICROMECHANICAL MODEL

Based on fracture mechanics and deformation mechanisms a micromechanical model will be used to control the failure mode of the fibre reinforced cementitious composite and predict the tensile strength by calculating the maximum bridging stress of a fibre reinforced cement matrix. The composite performance is described by micromechanical properties of the fibre-matrix system (Lin et al. 1999):

- Fibre parameters: fibre length (L_f), fibre diameter (d_f), fibre stiffness (E_f), fibre strength (σ_f), fibre volume fraction (V_f)
- Matrix parameters: matrix stiffness (E_m), matrix fracture toughness (K_m), initial flaw size (c).

- Fibre-matrix interaction parameters: interfacial frictional bond (τ_o), interfacial chemical bond (G_d), snubbing coefficient (f)

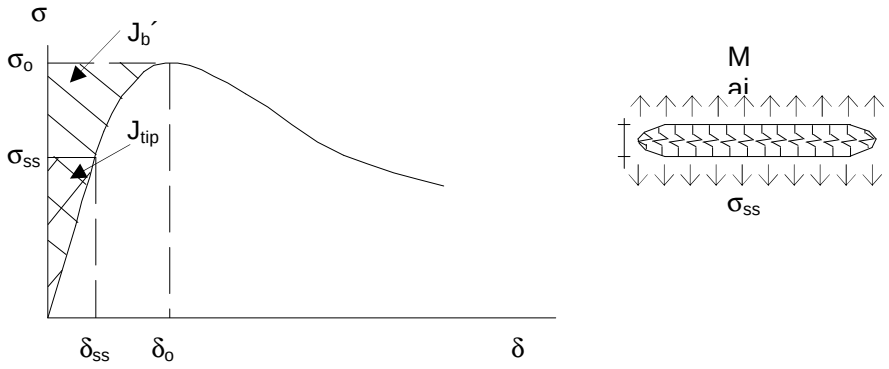

Fig. 1 Typical σ(δ) curve for strain-hardening composite

A material that shows a strain-hardening behaviour with multiple microcracking prior to failure develops enhanced ductility. Two criteria must be satisfied in order to achieve strain-hardening behaviour: steady state cracking criterion and first-crack stress criterion. The first one is an energy based criterion while the second one is a strength based criterion. The composite bridging law, also known as the stress-crack opening σ(δ) relation, is plotted in Fig. 1. This relation describes the fundamental material property that rules the mechanical performance of fibre reinforced composites beyond the first crack and can be formulated (Eq. 1) by integrating the contributing effects of the individual fibres bridging the crack. Eq. 1 takes into account probabilistic density functions, random orientation of fibres, fibre rupture, slip hardening and matrix spalling.

$$\sigma(\delta) = \frac{4V_f}{\pi d_f^2} \int_{\varphi=0}^{\pi/2} \int_{z=0}^{(L_f/2)\cos\varphi} P(\delta)\, p(\varphi)\, p(z)\, dz\, d\varphi \qquad (1)$$

$$J_{tip} \le \sigma_0 \delta_0 - \int_0^{\delta_0} \sigma(\delta)\, d\delta \equiv J_b' \qquad (2)$$

$$\sigma_{ss}\delta_{ss} - \int_0^{\delta_{ss}} \sigma(\delta)\, d\delta = J_{tip} \qquad (3)$$

$$J_b' = V_f \frac{L_f}{d_f}\left(\frac{\tau_0^{\,2} L_f^{\,2}}{6 d_f E_f} - 2G_d\right) \qquad (4)$$

The pullout load-displacement relation P(δ) is modelled at a single fibre level. P(δ) has two regions; first the debonding process that can be modelled as a tunnelling crack with a characteristic interface fracture energy G_d and after that the slip dominated by a constant frictional stress τ_o.

The steady state crack criterion will assure the presence of multiple cracking if the complementary energy J_b' is equal to, or greater than the matrix crack tip toughness J_{tip} (Eq. 3) estimated as K_m^2/E_m (Wang and Li 2007). J_b'depends on the fibre and fibre matrix interface parameters. It can be calculated from Fig. 1 (Eq. 2) and after some simplifications (Wang and Li 2007) it can then be derived as in Eq. 4. The concept of energy balance between external work, crack tip energy absorption and crack flank absorption energy during flat crack extension is used in Eq. 2.

The steady state crack stress σ_{ss} can be expressed as in Eq. 3.

The first-crack stress criterion states that the first crack strength σ_{fc} should not exceed the maximum bridging strength σ_o (Wu 2001). This criterion controls the initiation of cracks. σ_{fc} Is a function of the matrix fracture toughness K_m, internal flaw size and the σ(δ) relation.

WOOD FIBRES

Studies done by other researchers reported higher values of bending strength and toughness in wood fibre reinforced composites than for cement matrixes without them (Blackenhorn et al. 2001, Pehanich et al. 2004, Vares et al. 1997). The same studies showed a lower compressive strength for the reinforced samples, which was consistent with the higher water/cement ratio they had.

Spruce, larch and pine, three different types of softwood fibres were studied in this project. The two main species of trees are gymnosperms, another name for softwood or coniferous trees and angiosperms, also known as hardwood or broadleaf trees. Since softwood cells have a more simple form and there are no vessels, the percentage of fibres is higher than in hardwood, up to 90%, and the fibres tend to be more uniform this was the choice of fibres to work with. Furthermore the softwood fibres are longer (3 to 5 mm average) and thicker (up to 45 μm) than hardwood.

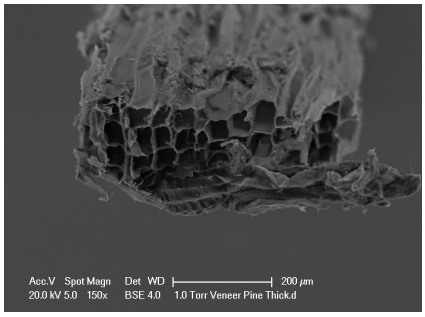

Fig. 1 – ESEM image of pine fibre

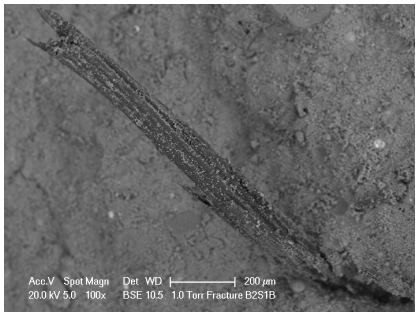

Fig. 2 – ESEM image of spruce fibre in a cement matrix

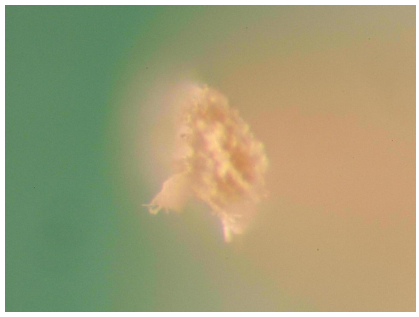

Fig. 3 – Light microscope image of tested larch fibre

The commercial price of wood fibres is 0.5 € per kilo, while the price of PVA fibres, one of the synthetic fibres currently used to reinforce cementitious matrixes is 12 € per kilo. Environmental costs are also considerably lower for wood and other natural fibres. Beside the fact that wood is a renewable resource these fibers need 70% less energy to be produced.

The fibres studied in this project are processed at Microlab. Small lumber blocks of larch and spruce (1x1x2 cm) are cooked following a neutral sulphite semichemical (NSSC) pulping procedure (Walker 2006) after which bundles of about 65 fibres are manually taken apart. On the other hand, pine wood bundles of about 160 fibres are cut from a veneer sheet using a microtome. Because of the production process, a full mechanical procedure, the pine bundles have rectangular shape and its cross section and size are more uniform from all the fibres studied (Fig. 1). The larch and spruce bundles, produced with a semi-chemical process, have a more rounded shape cross section, but the size and shape of it varied considerably from fibre to fibre (Fig. 2 and 3). The bundles are cut at length 10 mm. The bundles of fibres will now be referred to as fibres. As can be noticed in Fig. 1 to 3 wood fibres are hollow.

Table 1 – Average measured dimensional and mechanical properties of the wood fibres investigated

Fibre	Tensile strength σ_f [MPa]	Young´s modulus E_f [GPa]	Area [mm^2]
Spruce	663	39	0.055
Larch	708	34	0.041
Pine	730	29	0.113

Tensile strength of single wood fibres can be found in literature. It is then necessary to evaluate the tensile strength of the bundles of fibres proposed here as reinforcement. For that purpose the fibres were tested under direct tensile strength at the Microlab, using a micro tension-compression testing device (developed by Kammrath & Weiss) with a setup adapted for it (Fig. 4). The fibres are glued to two steel non-rotating

loading plates with a two component epoxy resin. The tests are performed under deformation control, using the deformation measured with a small extensometer (measuring length 10 mm), which is clamped onto the loading plates. The results from the tests are shown in Table 1. Some of these tests were done inside the Environmental Scanning Electron Microscope (ESEM) (Fig. 5 and 6). Lateral deformation of the fibres of less than 1% was observed during the tests, thus the Poisson ratio is null for these fibres.

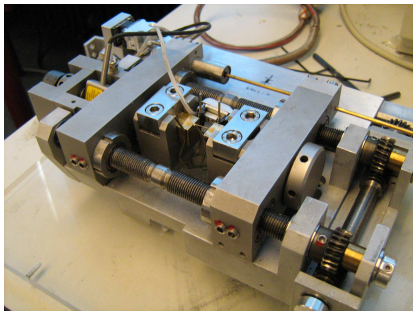

Fig. 4 – Single fibre tensile test setup

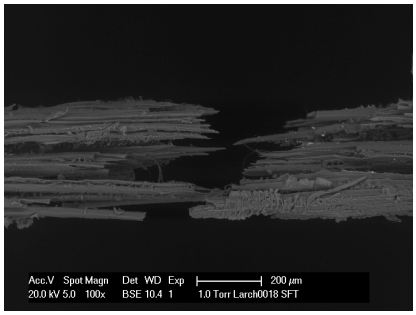

Fig. 5 – Larch fibre tested at ESEM

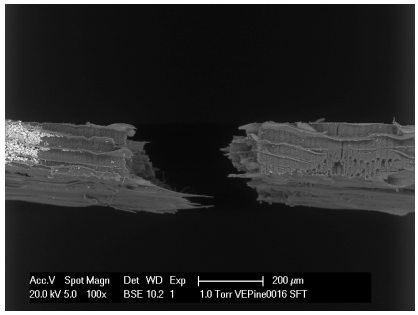

Fig. 6 – Pine fibre tested at ESEM

CEMENT MATRIX

Six different cement matrixes are proposed in this study whose mix proportions are given in Table 2. Mix 1 and 3 where prepared with sand which ranges from 0.125 – 0.25 mm and Mixes 4 to 6 with limestone powder (Zhou et al. 2008) with particle size of 13.41 µm. In all mixes cement type CEM I 52.5 N is used. Considering that cement production is energy-intensive: 5 % of global CO_2 emissions are due to cement production (WBCSD 2008) in this project cement is partially substituted with industrial by-products such as pulverized fly ash and blast furnace slag. This is done to achieve a more sustainable material. Fly ash is a coal combustion product (CCPs) which offers many environmental advantages, including its abundant availability, reducing energy investment in processing virgin materials and the use of a waste material. Blast furnace slag BSF is a non-metallic by-product from the manufacture of pig iron. Other options for greener materials may be Vitreous calcium alumino silicate VCAS which is a white pozzolan recycled from the waste from fibreglass manufacture or and Self cleaning cement SCC that contains a catalyst to trigger a reaction between organic pollutants in presence of UV rays.

The matrixes here studied have a water-to-dry-ingredients ratio between 0.26 for Mix 6 and 0.273 for Mixes 1 and 3.

The matrix fracture toughness K_m is measured from three or four point bending tests (Fig. 7 and 8). For a matrix with Mix 1 the matrix crack tip toughness J_{tip} is 15 J/m^2 (Wang and Li 2007). It was determined by a wedge splitting test in which vertical load applied on the wedge and crack opening at the loading position were recorded.

Table 2 - Mix proportions for Fibre pullout test

Mix ID	Cement	Fly Ash	Sand	BFSlag	Limestone	SP	Water
Mix 1	1	1.2	0.8			0.013	0.6
Mix 2	1	2.8				0.03	1
Mix 3	1		0.8	1.2		0.013	0.6
Mix 4	1			1.2	0.8	0.025	0.81
Mix 5	1			1.2	1.5	0.023	0.98
Mix 6	1			1.2	2	0.018	1.09

MATRIX-FIBRE INTERFACE

It is known that a strong chemical bond promotes fibre rupture: the fracture energy is reduced while the tensile strength of the composite increases, hence the material becomes strong but brittle. Since cement is an alkaline inorganic material (pH>12.5) containing surface hydroxyl groups (Coutts and Kightly 1984) and wood fibres contain covalent hydroxyl groups from residual lignin or both the cellulose component and the oxidation of end groups (Coutts and Kightly 1984, Pehanich et al. 2004) the chemical bond is believed to be either hydrogen bonds or hydroxide bridges between fibres or between the fibres and the cement matrix. This can be a strong chemical bond, so high values of G_d are expected (G_d>2).

To evaluate G_d and other fibre-matrix interface properties single fibre pullout tests are performed. A fibre with a controlled embedment length is pulled out from a block of matrix while the load vs displacement relation is recorded (Li et al. 2002). The embedment length of the specimen is chosen from 1 to 5 mm. Since shorter lengths ensure full debonding, the length is increased from 1 mm up to half the total fibre length (5mm in this case), maximum value for an embedment length. The pullout tests are conducted at speed of 0.002 mm/s on a MTS 810 testing machine (Fig. 12 to 14) in which the displacement of the test is given by the displacement of the actuator (±80 mm stroke) and the results data interpretation and calculation of the interface parameters will be done according to Lin et al.(1999). A 2-N load cell is used to measure the pullout forces of the fibres. The cement matrix sample is glue to a specimen mount plate and the free side of the fibre is glue to a fibre mounting plate. A free fibre length of 1 mm is left between plates.

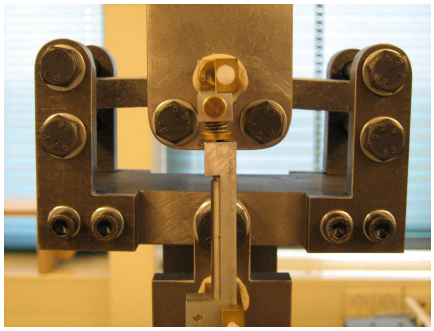

Fig. 7 –Four point bending test setup

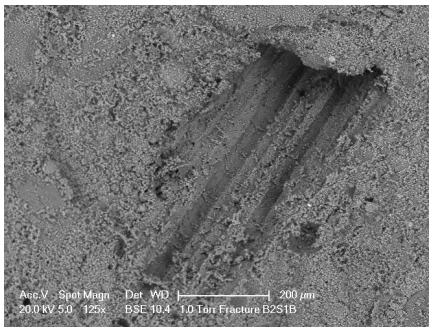

Fig. 8 – ESEM image of hole left by spruce fibre in cement matrix

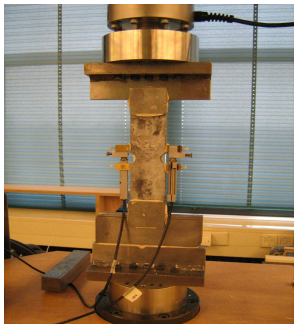

Fig. 9 – Direct tensile test setup

Fig. 10 shows a typical pullout curve for PVA fibre. After the first peak the load drops. From this difference in load the chemical debonding energy value G_d can be calculated. The raising portion of this curve, prior to the second peak, is interpreted as a slip-hardening effect. The same effect was observed in a pullout test with spruce fibre (Fig. 11), but as seen the second peak is lower than the first peak. In this case the maximum load is reached when both chemical and frictional bonds are acting, while with the PVA fibre, after loosing the chemical bonding the frictional bond increases while the fibre is pullout due to damage and jamming effect in the fiber. A slip hardening effect is desirable as it leads to an increased load resisting fiber pullout but it should not be too high in order to avoid fibre rupture. After the second peak the spruce fibre undergo with slip-softening effect.

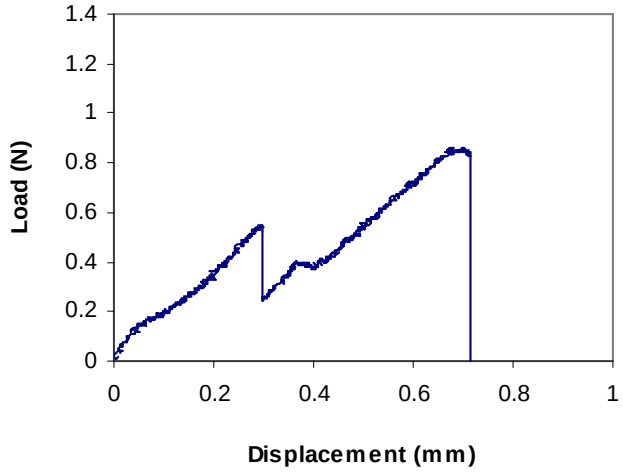

Fig. 10 – Pullout curve for PVA fibre and Mix 4

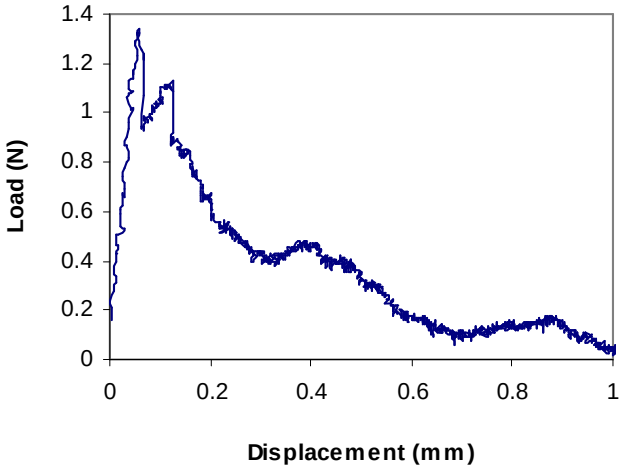

Fig.11 – Pullout curve for spruce fibre and Mix 4

The cement matrix from where the PVA fibre was pullout in the test shown in Fig. 10 is 0.7 mm thick and the cement matrix sample in the test in Fig. 11 is 1 mm thick. The spruce fibre has a cross section area about 18 times bigger than the PVA fibres. Considering the difference in embedment length in these two tests and the first peak pullout load in both cases the pullout peak stress before chemical debonding for the spruce fibre is 2.12 Mpa while for the PVA fibre is 6.14 Mpa. The samples were air cured and tested at age 28 days.

From Eq. 4 with the fibre properties mentioned in Table 1 and the assumed value of G_d>2 to assure a strain hardening behaviour ($J_b' > J_{tip}$) calculations show that the minimum values for τ_o should be as shown in Table 3. On the other hand if the matrix first crack strength σ_{fc} is higher than the here estimated values of σ_0 then after the first cracking of the cement matrix the fibers will not be able to sustain the load and the material will fail in a brittle mode. The maximum bridging strength σ_0 was estimated from deductions and formulations by Redon et al. (2001) and Wang and Li (2007).

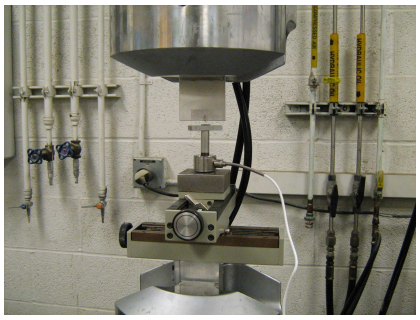

Fig. 12 – Pullout single fibre test setup

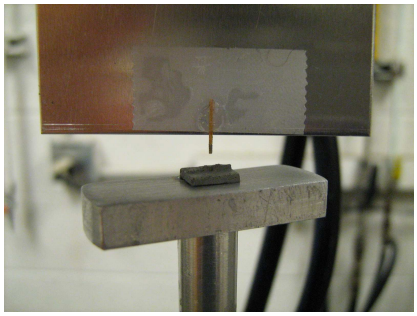

Fig. 13 – Detail of pullout test

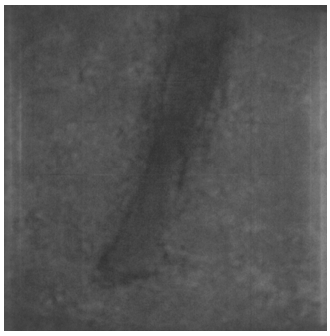

Fig. 14–CT-Scan of fibre in a cement matrix, a sample for pullout test

Fibre diameter has a strong influence in the estimation of J_b' A logical first assumption would be to lower the diameter of the fibres in order to be able to develop a ductile behaviour, but this may not be possible due to production constraints. Fibre length and volume fraction also have a strong impact in J_b' but high fibre percentage or longer fibres will decrease the reology of the composite, affecting the workability and the uniform dispersion of the fibres. Since the fibre aspect ratio is low (<100) there may be end effects on the total debonding load. The properties G_d and τ_o should be carefully studied as high values of τ_o suggest fibre rupture. The matrix contribution J_{tip} could be made lower by increasing the water to binder ratio, reducing the size of sand particles or by the use of inert filler.

Table 3 – Predicted values of τo and σo

	Spruce fibres		Larch fibres		Pine fibres	
Fibre vol. fraction	2%	4%	2%	4%	2%	4%
τ_o (Mpa) >	3.84	2.94	3.14	2.42	4.63	3.47
σ_o (MPa)	2.99	4.65	2.83	4.46	2.49	3.79

Table 3 presents rough estimates of the bridging strength calculated with equations derived by Wang and Li (2007) (for specific optimal conditions) and with the values of G_d and τ_o above mentioned. From direct tensile test on notched specimens (dimension: 170x35x10mm) (Fig. 9) performed at the Microlab the σ_{fc} for a composite with 2% by volume larch fibres is 3.4 MPa. During that test and in 4 point bending tests (Fig. 7) this composite did not develop strain hardening behaviour nor ductility. From Table 3 the σ_o for this composite is lower than σ_{fc} which means that after the first crack no more load is transferred, the load drops due to fibre rupture or pullout. To prevent this to happen the matrix strength should be lowered or ensure that the fibre matrix interaction parameters to and *Gd* be low.

ESEM micrographs of the fracture surface of composites with 2% spruce fibres tested at age 28 days show no dominating failure mode. Several fibres were pulled out (Fig. 2 and 8) but also fibres breakage was observed.

CONCLUSION AND FUTURE WORK

By relating microstructure to composite performance a micromechanics based design will help develop ductile wood fibres cementitious composites suitable for cast in place applications such as: structural elements in seismic design, lightweight elements, slurry walls, piles and plate foundations, floorings and concrete repair. To understand the interacting effects of fibre, matrix and the interfacial parameters will allow the designer to optimize the composition and take advantage of the unique characteristics of natural fibres. The first steps in developing this material are described in this paper. Future work in this ongoing project includes the development of new equations for the micromechanical model in which the shape of the fibres (not circular) will be taken into account and the evaluation of interfacial parameters for the proposed cement matrixes and possible modification of fibre surface through coating to assure the strain hardening behaviour of the reinforced cement matrix and full fibre-pullout of the fibres. Further studies to understand the time dependency of the chemical bond between fibres and matrix as well as understanding the effect of humidity on the properties of the fibres. Bending and direct tensile tests for wood fibre composites will be done in the future. The fibre distribution within the matrix will also be analyzed by using a CT-scanner, taking advantage of the difference in density between fibres and cement matrix.

ACKNOWLEDGEMENTS

The authors would like to acknowledge the financial support for this research from the National Council of Science and Technology (CONACYT), Mexico (Grant # 206108) and from INTRON. Furthermore the authors thank Prof. V. C. Li and Prof. K. Van Breugel for helpful discussions on the subject.

REFERENCES

Blankenhorn, P.R., Blankenhorn, B.D., Silsbee, M.R. and DiCola, M., 2001. "Effects of fiber surface treatments on mechanical properties of wood fiber-cement composites", *Cement and Concrete Research* 31, 1049-1055.

Coutts, R.S.P. and Kightly, P., 1984. "Bonding in wood fibre-cement composites", *Journal of Material Science* 19, 3355-3359.

de Lhoneux, B., Kalbskopf, R., Kim, P., Li, V.C., Lin, Z., Vidts, D., Wang, S. And Wu, H.C., 2002. "Development of high tenacity polypropylene fibers for cementitious composites". *In* "Proc., JCI Int. Workshop on Ductile fiber reinforced cementitious composites". Japan Concrete Institute, Japan.

Li, V.C., Wu, C., Wang, S., Ogawa, A., and Saito T., 2002. "Interface Tailoring for Strain-hardening PVA-ECC", *ACI Materials Journal* 99 (5) 463-472.

Lin, Z., Kanda, T. and Li, V.C., 1999. "On Interface Property Characterization and Performance of Fiber Reinforced Cementitious Composites", *J. Concrete Science and Engineering* 1, 173-184.

Pehanich, J.L., Blankenhorn, P.R. and Silsbee, M.R., 2004. "Wood fiber surface treatment level effects on selected mechanical properties of wood fiber-cement composites", *Cement Concrete Research* 34, 59-65.

Redon, C., Li, V. C., Wu, C., Hoshiro, H., Saito, T. and Ogawa, A., 2001. "Measuring and modifying interface properties of PVA fibers in ECC matrix", *Journal of Materials in Civil Engineering* 13 (6) 399-406.

Savastano Jr., H., 2000. *Materials using reinforced cement with vegetable fiber: recycling waste for low cost buildings*. PhD Thesis, University of Sao Paulo, Brazil.

Vares, S., Sarvaranta, L., and Lanu, M., 1997."Cellulose fibre concrete", *VTT Publication* 296.

Walker, J.C.F., 2006. "Pulp and paper manufacture". In "Primary wood processing principles and practice". Springer, Netherlands, 477-534.

Wang, S. and Li, V.C., 2007. "Engineered Cementitious Composites with High-volume Fly Ash", *ACI Material Journal* 104 (3) 233-241.

WBCSD World Business Council for Sustainable Development, 2008 [online]. Available from: http://www.wbcsd.org/templates/TemplateWBCSD5/layout.asp?MenuID=1

Wu, C., 2001. *Micromechanical tailoring of PVA-ECC for structural applications.* PhD Thesis, University of Michigan, Ann Arbor, USA.

Zhou, J., Qian, S., Sierra Beltran, M.G., Ye, G. and van Breugel, K., 2008. "Engineered cementitious composite with blast furnace slag and limestone powder". To be published in "Proceedings of the International Conference Microstructure Related Durability of Cementitious Composites". Nanjing.